ELSEVIER

Chemical Engineering Journal 106 (2005) 213–227

Chemical Engineering Journal

www.elsevier.com/locate/cej

A hybrid numerical approach for multi-responses optimization of process parameters and catalyst compositions in CO_2 OCM process over CaO-MnO/CeO_2 catalyst

Istadi[1], Nor Aishah Saidina Amin*

Chemical Reaction Engineering Group (CREG), Faculty of Chemical and Natural Resources Engineering, Universiti Teknologi Malaysia, UTM Skudai, Johor Bahru 81310, Malaysia

Received 21 July 2004; received in revised form 24 November 2004; accepted 2 December 2004

Abstract

A new hybrid numerical approach, using Weighted Sum of Squared Objective Functions (WSSOF) algorithm, was developed for multi-responses optimization of carbon dioxide oxidative coupling of methane (CO_2 OCM). The optimization was aimed to obtain optimal process parameters and catalyst compositions with high catalytic performances. The hybrid numerical approach combined the single-response modeling and optimization using Response Surface Methodology (RSM) and WSSOF technique of multi-responses optimization. The hybrid algorithm resulted in Pareto-optimal solutions and an additional criterion was proposed over the solutions to obtain a final unique optimal solution. The simultaneous maximum responses of C_2 selectivity and yield were obtained at the corresponding optimal independent variables. The results of the multi-response optimization could be used to facilitate in recommending the suitable operating conditions and catalyst compositions for the CO_2 OCM process.

Keywords: Weighted Sum of Squared Objective Functions; CO_2 OCM process; Multi-responses optimization; Pareto-optimal solutions

1. Introduction

The high CO_2/CH_4 ratio in Natuna's natural gas compositions, comprising of up to 71% carbon dioxide and 28% methane [1], should be strategically utilized for the production of higher hydrocarbons, liquid fuels and other important chemicals. Recently, the conversion of methane to C_2 hydrocarbons (ethane and ethylene) using carbon dioxide as an oxidant (carbon dioxide oxidative coupling of methane (CO_2 OCM)) has received considerable attention [2–9]. Eqs. (1) and (2) are the two main CO_2 OCM reaction schemes to produce C_2 hydrocarbons, while carbon monoxide and water are the by-products.

$$2CH_4 + CO_2 \rightleftharpoons C_2H_6 + CO + H_2O \qquad \Delta H^{\circ}_{298} = +106\,\text{kJ/mol} \tag{1}$$

$$2CH_4 + 2CO_2 \rightleftharpoons C_2H_4 + 2CO + 2H_2O \qquad \Delta H^{\circ}_{298} = +284\,\text{kJ/mol} \tag{2}$$

Catalyst screening of CeO_2-based catalysts for CO_2 OCM process over binary and ternary metal oxides [9] determined that the 15 wt.% CaO-5 wt.% MnO/CeO_2 catalyst as the most potential. Interestingly, the stability test showed that the 15 wt.% CaO-5 wt.% MnO/CeO_2 catalyst was stable with no obvious coking during 20 h of reaction time on stream. However, the process parameters and the catalyst compositions of the CO_2 OCM process have not been optimized.

* Corresponding author. Tel.: +607 5535588; fax: +607 5581463.
E-mail address: r-naishah@utm.my (N.A.S. Amin).
[1] Present address: Department of Chemical Engineering, Diponegoro University, Semarang 50239, Indonesia.

1385-8947/$ – see front matter © 2004 Elsevier B.V. All rights reserved.
doi:10.1016/j.cej.2004.12.001

The development of a highly efficient catalyst is important and the key to obtain a highly efficient catalyst is the catalyst design [10–13]. The relationships among catalyst compositions, process parameters and catalyst compositions toward the catalytic performances are very complex from the engineering and chemistry points of view, but the determination of a suitable catalyst is crucial for the CO_2 OCM process. Preferably, the very complex relation should be modeled at a molecular level in the catalyst design to obtain a suitable catalyst compositions and optimal operating conditions. The optimal operating parameters, such as the CO_2/CH_4 ratio and reactor temperature, and the catalyst compositions in the CeO_2-supported catalyst, provide essential information for industrial CO_2 OCM process.

Pertaining to the catalyst design, some previous researchers introduced artificial neural network (ANN) to design the catalysts [10–13]. The selection of optimization method is very important to design an optimal catalyst as well as the relations between process parameters and catalytic performances [14]. The previous researchers suggested that artificial neural network is feasible and many experiments can be avoidable [14]. According to the complex interaction among the catalyst compositions, the process parameters and the metal-support with no clear reaction mechanism in the CO_2 OCM process, it is more useful for the catalyst design using empirical models especially in the optimization studies. A single-response optimization is usually insufficient for the real CO_2 OCM process due to the fact that most responses, i.e. methane conversion, products selectivity and yield, are dependent. Therefore, simultaneous multi-responses technique combined with the statistical single-response modeling using RSM is superior. Empirical and pseudo-phenomenological modeling approaches have been employed by researchers [14–16] for optimizing the catalytic process. The empirical modeling is efficient for the catalytic process optimization, but the drawback is that the model does not describe the fundamental theory or actual phenomena. The empirical model may be more appropriate for process optimization when the kinetic mechanism is not well known.

Concerning the multi-responses optimization, a graphical multi-responses optimization technique was implemented for xylitol crystallization from synthetic solution [17], but it is not useful for more than two independent variables or highly non-linear models. In another study, a generalized distance approach technique was developed to optimize process variables in the production of protoplast from mycelium [18]. The optimization procedure was carried out by searching independent variables that minimize the distance function over the experimental region in the simultaneous optimal critical parameters. Recently, the robust and efficient technique of the elitist Non-dominated Sorting Genetic Algorithm (NSGA) was used to obtain the solution of the complex multi-objectives optimization problem [16,19–21]. A hybrid genetic algorithm (GA) with artificial neural network was also developed [16] to design optimal catalyst and operating conditions in the O_2 OCM process. In addition, a comprehensive optimization study of simulated moving bed process was also reported using a robust genetic algorithm optimization technique [22].

The main objective of this paper is to develop a new hybrid numerical approach for the simultaneous multi-responses optimization in the CO_2 OCM process. A key feature of the hybrid numerical approach is the development of the Weighting Sum of Squared Objective Functions (WSSOF) algorithm to the simultaneous maximization of two responses, i.e. CH_4 conversion and C_2 selectivity, CH_4 conversion and C_2 yield, or C_2 selectivity and C_2 yield, as the following task after the development of single-response models. In this hybrid numerical approach, the Nelder–Mead Simplex method was utilized in the algorithm for solving the unconstrained optimization problem.

2. Numerical methods and experimental design

2.1. Technique for single-response optimization

It is necessary to obtain the optimal single-response models and the corresponding independent variables before multi-responses optimization is carried out. The optimal single-responses are used for obtaining information of the optimization boundary ranges. For example, in multi-responses optimization, the simultaneous optimal C_2 selectivity and yield is resulted in the entire range between both individual optimal values. In addition, reactor temperature and CO_2/CH_4 ratio (process parameters) and wt.% CaO and wt.% MnO in the CeO_2 catalyst (catalyst compositions) are searched in the range between those of single-response optimization. It is supposed that the simultaneous optimum is located within the ranges of single-responses optimization. In this section, the single-response modeling and optimization are presented.

2.1.1. Design of experiment using central composite design

A Central Composite Rotatable Design (CCRD) for four independent variables was employed to design the experiments [26] in which the variance of the predicted response, Y, at some points of independent variables, X, is only a function of the distance from the point to the design center [23–25]. The design of experiment is intended to reduce the number of experiments and to arrange the experiments with various combinations of independent variables. In the rotatable design, the standard error, which depends on the coordinates of the point on the response surface at which Y is evaluated and on the coefficients β, is the same for all points that are the same distance from the central point. The value of α for rotatability depends on the number of points in the factorial portion of the design, which is given in Eq. (3) [23–25]:

$$\alpha = (F)^{1/4} \tag{3}$$

where F is the number of points in the cube portion of the design ($F = 2^k$, k is the number of factors). Since there are

Table 1
Experimental ranges and levels of factors or independent variables

Factors (X)	Range and levels (x_i)				
	$-\alpha$ (−2)	−1	0	+1	$+\alpha$ (+2)
CO_2/CH_4 ratio (X_1) (−)	1	1.5	2	2.5	3
Reactor temperature (X_2) (K)	973	1048	1123	1198	1273
wt.% CaO (X_3) (%)	5	10	15	20	25
wt.% MnO (X_4) (%)	1	3	5	7	9

four factors, the F number is equal to 2^4 (=16) points, while α is equal to $(16)^{1/4}$ (=2) according to Eq. (3).

Process parameters of CO_2/CH_4 ratio and reactor temperature, and catalyst compositions of wt.% CaO and wt.% MnO in the CeO_2-supported catalyst were selected as the independent variables. The ranges of the independent variables are based on the conditions screened prior to optimization and are often used in the literatures [4,5,7]. Pertaining to space velocity, gas hourly space velocity (GHSV) was fixed during the reaction. The fixed space velocity value was chosen based on the variables screening prior to optimization such that performance of the catalyst is not influenced significantly by the variable in the tested range. The ranges and levels used in the experiments are given in Table 1 in which X_1 denotes CO_2/CH_4 ratio, X_2 denotes reactor temperature, while X_3 and X_4 denote wt.% CaO and wt.% MnO in the CeO_2-supported catalyst, respectively [26]. In the experimental design, all variables are coded for statistical calculation according to Eq. (4) [23–25].

$$x_i = \frac{\alpha[2X_i - (X_{\max} + X_{\min})]}{X_{\max} - X_{\min}} \quad (4)$$

where x_i is the dimensionless coded value of the ith variable, X_i the natural value of the ith variable, $X_{\max}$ and $X_{\min}$ are the highest and the lowest limits of the ith variable, respectively.

The experimental design matrix resulted by the CCD revealed in Table 2 [26] consists of 26 sets of coded conditions expressed in natural values. The design consists of a two-level full factorial design ($2^4 = 16$), eight star points and two center points. Based on this table, the experiments for obtaining the responses, i.e. CH_4 conversion ($X(CH_4)$), C_2 hydrocarbons selectivity ($S(C_2)$) and C_2 hydrocarbons yield ($Y(C_2)$) are carried out at the corresponding independent variables addressed in the experimental design matrix. These experimental data

Table 2
Experimental design matrix in their natural values and experimental results

Run no.	Experimental design matrix of independent variables (uncoded)				Experimental results		
	CO_2/CH_4 ratio (X_1)	Reactor temperature (X_2)	wt.% CaO (X_3)	wt.% MnO (X_4)	$X(CH_4)$ (%)	$S(C_2)$ (%)	$Y(C_2)$ (%)
1	1.5	1048	10	3	2.63	69.01	1.82
2	1.5	1048	10	7	2.20	78.15	1.72
3	1.5	1048	20	3	1.76	24.62	0.43
4	1.5	1048	20	7	1.25	42.64	0.53
5	1.5	1198	10	3	7.95	32.71	2.60
6	1.5	1198	10	7	7.80	35.98	2.81
7	1.5	1198	20	3	9.92	27.84	2.76
8	1.5	1198	20	7	9.03	34.62	3.13
9	2.5	1048	10	3	2.68	60.20	1.61
10	2.5	1048	10	7	2.29	78.37	1.80
11	2.5	1048	20	3	2.92	55.95	1.63
12	2.5	1048	20	7	1.55	64.79	1.00
13	2.5	1198	10	3	9.74	18.73	1.82
14	2.5	1198	10	7	8.70	33.12	2.88
15	2.5	1198	20	3	13.41	16.21	2.17
16	2.5	1198	20	7	10.89	30.78	3.35
17	1	1123	15	5	2.27	70.51	1.60
18	3	1123	15	5	2.47	65.18	1.61
19	2	973	15	5	0.54	24.30	0.13
20	2	1273	15	5	16.59	14.32	2.38
21	2	1123	5	5	4.33	74.63	3.23
22	2	1123	25	5	3.70	66.30	2.45
23	2	1123	15	1	4.71	74.07	3.49
24	2	1123	15	9	4.53	75.24	3.41
25	2	1123	15	5	4.81	72.58	3.49
26	2	1123	15	5	5.06	75.64	3.83

Note: $X(CH_4)$, CH_4 conversion (%); $S(C_2)$, C_2 hydrocarbons selectivity (%); $Y(C_2)$, C_2 hydrocarbons yield (%); catalyst weight, 2 g; total feed flow rate, 100 ml/min; total pressure, 1 atm.

are used for validating the single-response model of the catalytic CO_2 OCM process. The sequence of experiment was randomized in order to minimize the effects of uncontrolled factors. Detail description of the single-response modeling, the catalyst preparation and the catalyst testing were reported elsewhere [26].

2.1.2. Single-response modeling using Response Surface Methodology (RSM)

The central composite design results revealed in Table 2 were analyzed using Response Surface Methodology. All single-responses were modeled using the RSM corresponded to independent variables [26]. The RSM is a technique consisting of [23–25]: (a) designing of experiments to provide adequate and reliable measurements of the response, (b) developing a mathematical model having the best fit to the data obtained from the experimental design, and (c) determining the optimal value of the independent variables that produces a maximum or minimum response. In this paper, the design of experiment and the Response Surface Methodology were employed using STATISTICA, version 6, software (StatSoft Inc., Tulsa, USA).

By the RSM, a quadratic polynomial equation was developed to predict the responses as a function of independent variables involving their interactions [23–25]. In general, the response for the quadratic polynomial is described in Eq. (5).

$$Y = \beta_0 + \sum_{j=1}^{4} \beta_j X_j + \sum_{j=1}^{4} \beta_{jj} X_j^2 + \sum_{i<j} \beta_{ij} X_i X_j \tag{5}$$

where Y is the predicted response, β_0 the intercept coefficient, β_j the linear terms, β_{jj} the squared terms, β_{ij} the interaction terms, and X_i and X_j represent the uncoded independent variables. The coefficients of the models for the three responses were estimated using multiple regression analysis technique included in the RSM. Fit quality of the models was judged from their coefficients of correlation and determination.

Pertaining to single-response optimization, the Nelder–Mead Simplex method was used to look for the optimal conditions in which each response variable achieved a maximum value. The single-response optimization produces a maximum CH_4 conversion, C_2 selectivity and C_2 yield independently with respect to a set of optimal process parameters and catalyst compositions.

2.1.3. Canonical analysis of stationary point

Vector $\boldsymbol{X}$ that maximizes the predicted responses is called the stationary point and comprises of X_1, X_2, X_3 and X_4. The stationary point exists such that the partial derivatives of predicted response over those points equal to zero. The stationary point could represent a point of maximum response, a point of minimum response or a saddle point. The part of the canonical analysis shows a nature of the stationary point [23–25]. In general, pertaining to the second order consideration, the model can be expressed in matrix notation as written in Eq. (6).

$$Y = \beta_0 + \boldsymbol{X}'\boldsymbol{b} + \boldsymbol{X}'\boldsymbol{B}\boldsymbol{X} \tag{6}$$

where

$$\boldsymbol{X} = \begin{bmatrix} X_1 \\ X_2 \\ X_3 \\ X_4 \end{bmatrix}, \quad \boldsymbol{b} = \begin{bmatrix} \beta_1 \\ \beta_2 \\ \beta_3 \\ \beta_4 \end{bmatrix} \quad \text{and}$$

$$\boldsymbol{B} = \begin{bmatrix} \beta_{11} & \frac{\beta_{12}}{2} & \frac{\beta_{13}}{2} & \frac{\beta_{14}}{2} \\ \frac{\beta_{21}}{2} & \beta_{22} & \frac{\beta_{23}}{2} & \frac{\beta_{24}}{2} \\ \frac{\beta_{31}}{2} & \frac{\beta_{32}}{2} & \beta_{33} & \frac{\beta_{34}}{2} \\ \frac{\beta_{41}}{2} & \frac{\beta_{42}}{2} & \frac{\beta_{43}}{2} & \beta_{44} \end{bmatrix} \quad \text{for } \beta_{ij} = \beta_{ji}$$

The stationary point can be calculated in Eq. (7).

$$\boldsymbol{X}_0 = -\tfrac{1}{2}\boldsymbol{B}^{-1}\boldsymbol{b} \tag{7}$$

The predicted response at the stationary point is approximated in Eq. (8).

$$Y_0 = \beta_0 + \tfrac{1}{2}\boldsymbol{X}_0'\boldsymbol{b} \tag{8}$$

The characteristic of the stationary point at the critical response is determined from the sign and magnitude of the eigenvalues (λ_i) [23,25,27]. The eigenvalues are obtained from the roots of the determinant relation as given in Eq. (9).

$$|\boldsymbol{B} - \lambda \boldsymbol{I}| = 0 \tag{9}$$

If the λ_i are all positive, then $\boldsymbol{X}_0$ is a point of minimum response; if the λ_i are all negative, then $\boldsymbol{X}_0$ is a point of maximum response [25,27]. However, if the λ_i have different signs, $\boldsymbol{X}_0$ is a saddle point. Transformation of the fitted model into a new coordinate system with the origin at the stationary point $\boldsymbol{X}_0$ and thus rotation of the axes until they are parallel to the principal axes help to characterize the stationary point of the fitted models [23–25]. An equation developed by the transformation is called the canonical form of the model, which is given in Eq. (10)

$$Y = Y_0 + \lambda_1 w_1^2 + \lambda_2 w_2^2 + \lambda_3 w_3^2 + \lambda_4 w_4^2 \tag{10}$$

where w_i ($i = 1, 2, 3, 4$) denotes the transformed independent variables or the canonical variables.

2.2. Theory for multi-responses optimization

In fact, there is a vector of objectives, $\boldsymbol{F}(\boldsymbol{X}) = \{F_1(\boldsymbol{X}), F_2(\boldsymbol{X}), \ldots, F_M(\boldsymbol{X})\}$ where M denotes the number of objectives, that must be considered in chemical engineering process. The optimization techniques are developed to

find a set of decision parameters, $\boldsymbol{X} = \{X_1, X_2, \ldots, X_N\}$ where N is the number of independent variables, defined as the optimal independent variables. As the number of responses increases, the optimal solutions are likely to become complex and less easily quantified. Therefore, the development of multi-responses optimization strategy enables a numerically solvable and realistic design problem [14,28].

The task in multi-responses optimization is to create a non-inferior solution to a set of problems and then select among its members a solution that satisfies the objectives [22,29]. Generally, the mathematical description of multi-responses optimization is concerned with the minimization or maximization of a vector of objective functions, $\boldsymbol{F}(\boldsymbol{X})$, subject to a number of constraints and/or bounds as defined in Eq. (11) [27,29–30].

$$\begin{aligned} &\underset{\boldsymbol{X}\in\Re^N}{\text{minimize}} \quad \boldsymbol{F}(\boldsymbol{X}) = [F_1(\boldsymbol{X}), F_2(\boldsymbol{X}), \ldots, F_M(\boldsymbol{X})]^{\mathrm{T}} \\ &\text{subject to :} \quad G_i(\boldsymbol{X}) = 0, \qquad i = 1, \ldots, I \\ &\qquad\qquad\quad H_j(\boldsymbol{X}) \le 0, \qquad j = 1, \ldots, J \\ &\qquad\qquad\quad X_k^{\mathrm{L}} \le X_k \le X_k^{\mathrm{U}}, \quad k = 1, \ldots, N \\ &\qquad\qquad\quad M \ge 2 \end{aligned} \tag{11}$$

In this problem there are N variables with J inequality constraints and I equality constraints. The function vector $\boldsymbol{F}(\boldsymbol{X})$ is the objective functions, $G_i(\boldsymbol{X})$ the ith equality constraints and $H_j(\boldsymbol{X})$ is the jth inequality constraints. The kth variable is varied in the bounds of $[X_k^{\mathrm{L}}, X_k^{\mathrm{U}}]$. The objective space means the space to which the objective vector belongs. The set of all feasible points $\boldsymbol{X}$ is called the feasible region $\boldsymbol{F}$, but in fact, there is no unique solution to this problem if any of the components of $\boldsymbol{F}(\boldsymbol{X})$ are competing. The multi-responses optimization concept is subsequently defined more precisely by considering a feasible region (Ω) for the parameter space ($\boldsymbol{X} \in \Re^N$) that satisfies all the constraints as written in Eq. (12) [27,30].

$$\begin{aligned} &\Omega = \{\boldsymbol{X} \in \Re^N\} \\ &\qquad\qquad G_i(\boldsymbol{X}) = 0, \qquad i = 1, \ldots, I \\ &\text{subject to :} \quad H_j(\boldsymbol{X}) \le 0, \qquad j = 1, \ldots, J \\ &\qquad\qquad X_k^{\mathrm{L}} \le X_k \le X_k^{\mathrm{U}}, \quad k = 1, \ldots, N \end{aligned} \tag{12}$$

The formulation allows us to define the corresponding feasible region (Λ) for the objective function space ($\boldsymbol{F} \in \Re^M$) as formulated in Eq. (13).

$$\begin{aligned} &\Lambda = \{\boldsymbol{F} \in \Re^M\} \quad \text{where } \boldsymbol{F} = \boldsymbol{F}(\boldsymbol{X}) \\ &\text{subject to :} \quad \boldsymbol{X} \in \Omega \end{aligned} \tag{13}$$

The mapping of the parameter space (Ω) into the objective function space (Λ) represented for a two-dimensional case is depicted in Fig. 1(a) [30]. Therefore, a non-inferior solution is defined from the feasible region of objective function space (Λ) within the parameter space of individual objective functions of $\boldsymbol{F}(\boldsymbol{X})$. The solutions are known as Pareto-optimal or non-dominated solutions. A vector $\boldsymbol{X}^* \in \Omega$ is said

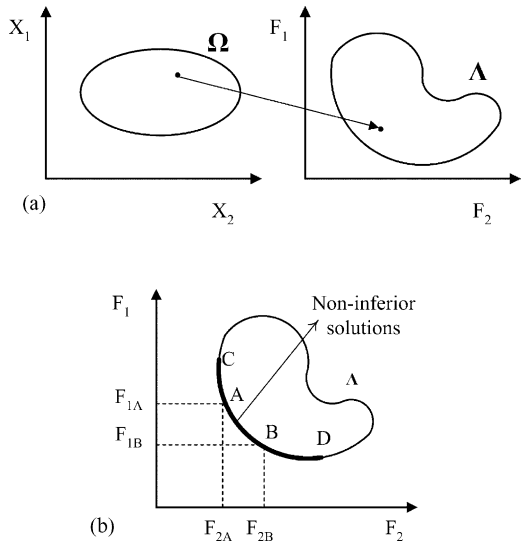

Fig. 1. Technique for solving multi-response optimization problem: (a) mapping from parameter space (Ω) into objective function space (Λ); (b) Pareto-optimal solutions.

to be a Pareto-optimal point or a non-inferior solution point for multi-responses optimization if and only if there is no $\boldsymbol{X} \in \Omega$ such that $F_M(\boldsymbol{X}) \le F_M(\boldsymbol{X}^*)$ for all $M \in \{1, 2, \ldots, M\}$ for minimization. A Pareto set is defined such that when we move from one point to another, at least one objective function improves and at least one other worsens. In the two-dimensional illustration, the set of non-inferior solution is depicted in Fig. 1(b) in which the Pareto-optimal solution points lie on the curve between points C and D. Points A and B represent a specific non-inferior solution points because an improvement in one objective, F_1, requires an increment in the other objective, F_2, such that $F_{1\mathrm{B}} < F_{1\mathrm{A}}$ and $F_{2\mathrm{B}} > F_{2\mathrm{A}}$.

Several methods are available for solving multi-responses optimization problem, for example, weighted sum strategy [30–32], ε-constraint method [28,30,31,33], goal attainment method [28,30] and Non-dominated Sorting Genetic Algorithm [19,22,28] to obtain the Pareto set. Among the methods, the NSGA is the most powerful method for solving a complex multi-responses optimization problem. In the optimization of CO_2 OCM process, the WSSOF method is proposed to solve the optimization of process parameters and catalyst composition in combination with the Response Surface Methodology.

Particularly, the multi-responses optimization problem, described in Eq. (11), can be formulated by converting the problem into a scalar single-response optimization problem, $f(\boldsymbol{X})$, which is easy to be solved using unconstrained single-response optimization technique. The WSSOF technique allows a simpler algorithm, but unfortunately, the solution obtained depends largely on the values assigned to the weighting factors chosen. The scalar single-response equation converted from multi-responses optimization problem is expressed in Eq. (14) [21,27,30–31,34], which con-

siders the Weighted Sum of Squared Objective Functions method [32]:

$$\begin{aligned} &\underset{\boldsymbol{X}\in\Omega}{\text{maximize}} \quad f(F_i, W_i) = \sum_{i=1}^{2} W_i \cdot F_i(\boldsymbol{X})^2 \\ &\text{subject to}: \quad \sum_{i=1}^{2} W_i = 1 \quad \text{and} \quad 0 \le W_i \le 1 \end{aligned} \tag{14}$$

where $f(F_i,W_i)$ is called the utility function and the parametric weighting factors (W_i) are under the constraint set (Ω). Generally, multi-responses optimization studies try to find the best tradeoff among more than one objective or to calculate all non-inferior solutions.

In the equations, W_1 and W_2 denote weighting factors with respect to the objective functions, $F_1(\boldsymbol{X})$ and $F_2(\boldsymbol{X})$, respectively. The coupled responses, i.e. C_2 selectivity and C_2 yield, CH_4 conversion and C_2 selectivity, or CH_4 conversion and C_2 yield, are assigned to the objective functions, $\boldsymbol{F}(\boldsymbol{X})$, and the problem lies in attaching the weighting factors to each objective function. The weighting factors do not necessarily correspond directly to the relative importance of the objective functions. The maximization of Eq. (14) is interpreted as selection of W_1 and W_2 weighting factors for which the slope of the line comprising the weighting factors leads to the solution point where the line touches the boundary of Λ. The underlying problem is that there are many combinations of W_1 and W_2 values to convince the non-inferior solution point.

2.3. Additional criterion for determination of final optimal responses

Theoretically, all sets of non-inferior solutions at corresponding weighting factors are acceptable. In a real process, it is recommended to choose a set of operating conditions that will be adjusted to get high catalytic performances. In fact, the sets of solutions are not the final solution of the process optimization problem. The subsequent task of the non-inferior solutions is the selection of final optimal criterion, which requires an additional knowledge about the system. In this case, the sum of the objective functions, $\sum\boldsymbol{F}(\boldsymbol{X})$, is proposed as the final optimal criterion in the CO_2 OCM optimization. The idea is based upon the main objective that the responses are maximized simultaneously. For example, in the multi-responses optimization of C_2 selectivity and yield of the CO_2 OCM process, the maximum C_2 selectivity and yield are desired. It is supposed that when C_2 selectivity and yield achieved their maximum values simultaneously, sum of both responses also achieved maximum. In this case, the variation of weighting factors allows the generation of corresponding C_2 selectivity and yield values with respect to the non-inferior solutions. The additional criterion is developed by summing both normalized responses which in turn the pair data of weighting factors, normalized responses and sum of the normalized responses are generated. The normalization of each response can be performed by employing Eq. (15).

$$\hat{\boldsymbol{F}}_1 = \frac{F_1 - F_1^{\mathrm{L}}}{F_1^{\mathrm{U}} - F_1^{\mathrm{L}}}, \qquad \hat{\boldsymbol{F}}_2 = \frac{F_2 - F_2^{\mathrm{L}}}{F_2^{\mathrm{U}} - F_2^{\mathrm{L}}} \tag{15}$$

The next task is choosing a maximum point of the generated $\sum\hat{\boldsymbol{F}}_i$ data with respect to maximum responses simultaneously. At this condition, the optimal independent variables are attained. The corresponding optimal weighting factors, responses, and independent variables are determined by interpolation technique.

2.4. Algorithm of WSSOF technique in multi-responses optimization

In this case, the multi-responses optimization utilizes the single-response models developed by the RSM [26]. The boundary limits in the multi-responses optimization are determined by minimizing the responses independently in single-response optimization. The detail single-response model development using the RSM was reported elsewhere [26]. The Nelder–Mead Simplex method was used in single-response optimization using MATLAB codes.

Basically, the multi-responses optimization deals with the generation and selection of non-inferior solution points or Pareto-optimal solutions. The techniques for multi-responses optimization are wide and various. In this paper, the weighted sum of square objective functions is developed. The WSSOF converts the multi-responses problem into a scalar single-response one by creating a weighted sum of square of all the response functions as mentioned in Eq. (14) [21,27,30–32,34].

Detail of the WSSOF algorithm in the multi-responses optimization can be stated as follows:

Step 1. Develop the independent response models ($F_1(\boldsymbol{X})$ and $F_2(\boldsymbol{X})$) using Response Surface Methodology supported by the number of experimental data.

Step 2. Get values of maximum of the responses by minimizing the models independently of each other using Nelder–Mead Simplex algorithm. This step is aimed to obtain the boundary limits of multi-responses. In this step:

- maximize$_{X\in\Omega}$ $F_1(\boldsymbol{X}) = F_1^{\mathrm{U}}(\boldsymbol{X}^*)$, at this optimum point $F_2(\boldsymbol{X}^*) = F_2^{\mathrm{L}}(\boldsymbol{X}^*)$;
- maximize $_{X\in\Omega}$ $F_2(\boldsymbol{X}) = F_2^{\mathrm{U}}(\boldsymbol{X}^*)$, at this optimum point $F_1(\boldsymbol{X}^*) = F_1^{\mathrm{L}}(\boldsymbol{X}^*)$.

Step 3. Formulate a multi-responses optimization problem by utilizing the single-response models according to Eq. (11).

$$\underset{\boldsymbol{X}\in\Re^N}{\text{maximize}} \quad \boldsymbol{F}(\boldsymbol{X}) = F_i(\boldsymbol{X})$$

Step 4. Convert the multi-responses optimization problem in Step 3 into a single-response optimization problem by introducing weighting factors, W_i, according to Eq. (14).

$$\underset{\boldsymbol{X}\in\Omega}{\text{maximize}} \quad f(F_i, W_i) = \sum_{i=1}^{2} W_i \cdot F_i(\boldsymbol{X})^2$$

$$\text{subject to :} \quad \sum_{i=1}^{2} W_i = 1 \quad \text{and} \quad 0 \le W_i \le 1$$

Step 5. Solve the generated scalar single-response optimization problems using unconstrained optimization technique with respect to the variation of the weighting factor (W_i). Boundary limits of the searching are based on the results of Step 2. Use the Nelder–Mead Simplex technique for multi-variable unconstrained optimization to solve the scalar single-response optimization. Find the solution of $\boldsymbol{X}^*$ and $\boldsymbol{F}(\boldsymbol{X})$ values corresponding to each combination of W_i subject to $\sum W_i = 1$, and $W_i \ge 0$. The detail sub-algorithm for this step can be written as follows:

Step 5a. Pick a starting point $\boldsymbol{X}_0$. Set initial $W_i = [0\ 1]^{\mathrm{T}}$ means that the searching is started from the boundaries $F_2(\boldsymbol{X}^*) = F_2^{\mathrm{U}}(\boldsymbol{X}^*)$ and $F_1(\boldsymbol{X}^*) = F_1^{\mathrm{L}}(\boldsymbol{X}^*)$.

Step 5b. Put the scalar single-response model of Eq. (14) as a function file.

Step 5c. Solve the scalar single-response unconstrained optimization problem (Eq. (14)) in Step 5b using Nelder–Mead Simplex technique. This step produces the optimal values of $\boldsymbol{X}^*$, $F_1(\boldsymbol{X}^*)$ dan $F_2(\boldsymbol{X}^*)$ with respect to the variation of weighting factor W_i.

Step 5d. Calculate the normalized optimal responses values ($\hat{F}_1(\boldsymbol{X}^*)$ and $\hat{F}_2(\boldsymbol{X}^*)$) according to Eq. (15). Calculate sum of both normalized responses values: ($\Sigma\hat{\boldsymbol{F}}(\boldsymbol{X}^*) = \hat{F}_1(\boldsymbol{X}^*) + \hat{F}_2(\boldsymbol{X}^*)$).

Step 5e. Is $W_1 \le 1$? If yes, update W_i values and go to Step 5b. If no, terminate.

Step 6. Select a maximum value of the sum of normalized responses at each W_i variations.

Step 7. Get the corresponding values of $\boldsymbol{X}^*$, $F_1(\boldsymbol{X}^*)$ and $F_2(\boldsymbol{X}^*)$ using interpolation method.

In this algorithm, the single-response optimization problem can be solved using a standard unconstrained optimization algorithm of Nelder–Mead Simplex technique [35], which is a robust algorithm for problems that are very nonlinear or have a number of discontinuities.

3. Results and discussions

3.1. Single-response optimization of CO_2 OCM process

The empirical single-response modeling of CO_2 OCM process over CaO-MnO/CeO_2 catalyst was developed by RSM based on design of experiment using CCRD. The models of CH_4 conversion, C_2 hydrocarbon selectivity and yield were developed as a function of the process parameters, i.e. CO_2/CH_4 ratio (X_1), reactor temperature (X_2), and the catalyst compositions, i.e. wt.% CaO (X_3) and wt.% MnO (X_4). The models of CH_4 conversion, C_2 hydrocarbons selectivity and yield were described in Eqs. (16–18), respectively [26].

$$\begin{aligned} F_{\mathrm{CH_4\ conversion}}(\boldsymbol{X}) = {} & 230.9612 - 4.1100X_1 - 0.4251X_2 \\ & - 2.1151X_3 + 1.2208X_4 - 1.8843X_1^2 \\ & + 0.0002X_2^2 - 0.0024X_3^2 + 0.0232\ X_4^2 \\ & + 0.0107X_1X_2 + 0.0995X_1X_3 \\ & - 0.2087X_1X_4 + 0.0019X_2X_3 \\ & - 0.0008X_2X_4 - 0.0204X_3X_4 \end{aligned} \tag{16}$$

$$\begin{aligned} F_{\mathrm{C_2\ selectivity}}(\boldsymbol{X}) = {} & -3480.035 + 177.6118X_1 + 6.3335X_2 \\ & - 16.6266X_3 + 11.9748X_4 \\ & - 15.6574X_1^2 - 0.0029X_2^2 - 0.1304X_3^2 \\ & - 0.5532X_4^2 - 0.1286X_1X_2 \\ & + 1.5858X_1X_3 + 1.172X_1X_4 \\ & + 0.0144X_2X_3 - 0.0063X_2X_4 \\ & + 0.0202X_3X_4 \end{aligned} \tag{17}$$

$$\begin{aligned} F_{\mathrm{C_2\ yield}}(\boldsymbol{X}) = {} & -150.0778 + 12.7327X_1 + 0.2579X_2 \\ & - 0.6948X_3 - 1.3511\ X_4 - 2.2464X_1^2 \\ & - 0.0001X_2^2 - 0.0101X_3^2 - 0.0250X_4^2 \\ & - 0.0044X_1X_2 + 0.0536X_1X_3 \\ & + 0.0754X_1X_4 + 0.0008\ X_2X_3 \\ & + 0.0014X_2X_4 - 0.0021X_3X_4 \end{aligned} \tag{18}$$

In the methane conversion model, Eq. (16), the regression coefficients are estimated with a satisfactory determination coefficient (R^2) of 0.975. The methane conversion model has a considerable fitness between the experimental and the predicted values. Meanwhile, the regression coefficients of C_2 hydrocarbons selectivity model, Eq. (17), are estimated with adequate determination coefficient (R^2) of 0.803 indicates a fairly good agreement between the experimental and the predicted values. The C_2 hydrocarbons yield model stated in Eq. (18) with R^2 of 0.952 implies a reasonable fit between the experimental and the predicted values. The model is valid in the range of operating conditions described previously [26].

Table 3
Independent optimal values of C_2 hydrocarbons selectivity from single-response optimization

Independent variables ($\boldsymbol{X}$)	Location of optimum	Maximum C_2 selectivity (%)
CO_2/CH_4 ratio (X_1)	1.9	
Reactor temperature (X_2) (K)	1080	82.62
wt.% CaO in the catalyst (X_3) (%)	8.2	
wt.% MnO in the catalyst (X_4) (%)	6.8	

The canonical analysis based on the stationary point of the CH_4 conversion, C_2 hydrocarbons selectivity and yield model are revealed in Eqs. (19)–(21), respectively.

$$Y_1 = 2.756 - 1.8913w_1^2 - 0.006w_2^2 + 0.0003w_3^2 + 0.0337w_4^2 \quad (19)$$

$$Y_2 = 82.6022 - 15.7206w_1^2 - 0.5343w_2^2 - 0.0866w_3^2 - 0.0024w_4^2 \quad (20)$$

$$Y_3 = 11.8116 - 2.2474w_1^2 - 0.0244w_2^2 - 0.0098w_3^2 - 0.0001w_4^2 \quad (21)$$

where Y_1, Y_2, and Y_3 stand for the canonical form of the CH_4 conversion, C_2 selectivity and yield models, respectively. The mixed or different eigenvalues signs in Eq. (19) indicate that the CH_4 conversion model has a shape like a saddle at the stationary point [26,27], which consequently does not present a unique optimum point. The different trend is shown by C_2 selectivity and yield models in Eqs. (20) and (21), respectively. Both models show all negative eigenvalues indicate a unique maximum C_2 selectivity at the stationary point. The different magnitudes of eigenvalues reveal an elliptical contour shape, which means the effect of interaction among the independent variables is important [27].

The multi-variables single-response optimization was performed using the Nelder–Mead Simplex technique. Tables 3 and 4 reveal the independent optimal values of C_2 hydrocarbon selectivity and yield responses, respectively, together with their optimal independent variables. From Table 3, the C_2 hydrocarbons selectivity achieves a maximum value of 82.62% at the corresponding optimal factors of CO_2/CH_4 ratio, reactor temperature, wt.% CaO and wt.% MnO being 1.9, 1080 K, 8.2% and 6.8%, respectively. The results of the single-response optimization [26] is closed to the result by Wang et al. [5,7] and Cai et al. [8] in which a high C_2 selectivity was achieved at lower reactor temperature and high CO_2/CH_4 ratio (about 2). In addition, the maximum C_2 hydrocarbons yield is attained at 3.93% with respect to CO_2/CH_4 ratio, reactor temperature, wt.% CaO and wt.% MnO of 2.0, 1175 K, 15.3% and 7.3%, respectively, as revealed in Table 4. The optimal C_2 yield was achieved at higher reactor temperature (1123–1148 K) and high CO_2/CH_4 ratio (about 2), which is in agreement with other researchers results [5,7,8]. The subsequent task of this work is focused on finding the simultaneous maximum values of both responses.

Table 4
Independent optimal values of C_2 hydrocarbons yield from single-response optimization

Independent variables ($\boldsymbol{X}$)	Location of optimum	Maximum C_2 yield (%)
CO_2/CH_4 ratio (X_1)	2.0	
Reactor temperature (X_2) (K)	1175	3.93
wt.% CaO in the catalyst (X_3) (%)	15.3	
wt.% MnO in the catalyst (X_4) (%)	7.3	

3.2. Interpretation of multi-responses optimization technique

3.2.1. A hybrid numerical approach of WSSOF technique

Basically, the relation between catalysts compositions, process parameters and the catalytic reaction performances cannot be described in a simple empirical mathematical model. The mathematical models for CH_4 conversion, C_2 selectivity and yield are complex that depend on the catalyst composition and operating conditions, etc. The empirical modeling using RSM combined with multi-responses optimization is useful for optimizing the CO_2 OCM process in certain ranges of independent variables before the kinetic studies are carried out, but the models may be meaningless physically and phenomenologically. The hybrid method is also useful for exploring the interaction between the variables towards the process performances. The empirical modeling and the multi-responses optimization method are useful for designing a catalyst composition in relation with the process parameters and validated with some experimental data. The results of the hybrid multi-responses optimization can be used to recommend the operating conditions and catalyst compositions for further experimental works in CO_2 OCM process especially in the kinetic studies.

A numerical approach is implemented in this paper to optimize the simultaneous responses over the independent variables. The single-response modeling and optimization were conducted prior to multi-responses optimization using the Response Surface Methodology and the Nelder–Mead Simplex technique, respectively. The hybrid numerical approach combines the single-response modeling using RSM and solving the multi-responses optimization using WSSOF technique. Meanwhile, an additional criterion was proposed to obtain a final unique solution. In the multi-responses optimization, the numerical WSSOF technique is proposed by converting the multi-responses optimization into a scalar single-response problem as aforementioned in Eq. (14).

The detail numerical algorithm for the multi-responses optimization using the WSSOF technique was described clearly in the previous section. The numerical technique can be treated by introducing the weighting factors, W_1 and W_2, corresponding to $F_1(\boldsymbol{X})$ and $F_2(\boldsymbol{X})$, respectively. The two weighting factors do not necessarily correspond directly to the relative importance of the objectives. Sets of non-inferior solution points or Pareto-optimal solutions are obtained. In a

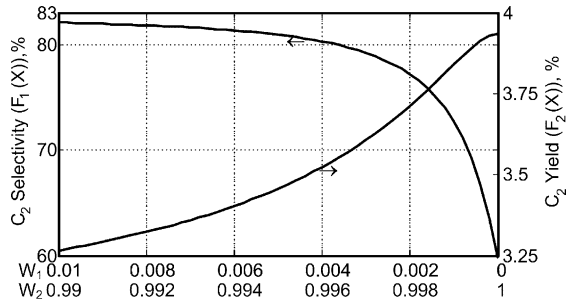

Fig. 2. Relationship of weighting factors variation and objective functions (C_2 selectivity and yield) in Pareto-optimal solutions.

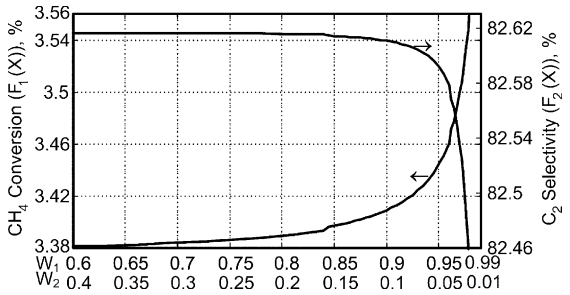

Fig. 3. Relationship of weighting factors variation and objective functions (CH_4 conversion and C_2 selectivity) in Pareto-optimal solutions.

non-inferior solution set, no decrease can be made in any of the objectives without causing a simultaneous increase in one or more of the other objectives. One of the weighting factors (W_1) corresponding to $F_1(\boldsymbol{X})$ is varied in the range of 0–1, while another (W_2) with respect to $F_2(\boldsymbol{X})$ is varied conversely between 1 and 0 according to the constrain that sum of W_1 and W_2 equal to 1 [32]. Each weighting factor variation produces a scalar single-response optimization problem, which resulted in an optimal response corresponding with optimal decision variables ($\boldsymbol{X}$). These treatments give a set of solution points or Pareto-optimal solution after whole weighting factor was varied.

In fact, the non-inferior solution points at corresponding weighting factors variation are not the final solution of the problem. It is still difficult to recommend a set of operating conditions and catalyst compositions that are suitable to achieve a high C_2 selectivity and yield simultaneously. The subsequent selection of those non-inferior solution points for a unique optimal solution requires a final decision criterion, which needs additional knowledge about the system. In this case, sum of the objective functions, $\sum \boldsymbol{F}(\boldsymbol{X})$, is proposed as the final optimal criterion in the CO_2 OCM process optimization. As a result, the final optimal values of the responses corresponding to the optimal independent variables are generated.

3.2.2. *Effect of weighting factors variation to the Pareto-optimal solution points*

Generally, the multi-responses optimization attempts to find the best tradeoff among more than one objective or to calculate all non-inferior solutions. In this case, the effect of weighting factors variations are shown in Figs. 2–4 pertaining to the simultaneous optimization of C_2 selectivity and yield, CH_4 conversion and C_2 selectivity, and CH_4 conversion and C_2 yield, respectively.

Fig. 2 takes into account the variation effect of W_1 and W_2 to the objective functions ($\boldsymbol{F}(\boldsymbol{X})$) of C_2 selectivity and yield at which W_1 is varied in the range of 0.01–0, while consequently W_2 is varied in the range of 0.99–1. It is shown that increasing W_1 from 0 to 0.01 at decreased W_2 from 1 to 0.99 leads to increased objective function value of C_2 selectivity, $F_1(\boldsymbol{X})$, and simultaneously decreases C_2 yield, $F_2(\boldsymbol{X})$. The zero value of W_1 and the unity value of W_2 during the multi-responses optimization mean a single-response optimization of $F_2(\boldsymbol{X})$ as revealed in the algorithm of Step 2. Meanwhile on the contrary, the unity value of W_1 and the zero value of W_2 during the multi-response optimization mean an individual response optimization of $F_1(\boldsymbol{X})$. This phenomenon is formulated in Step 2 of WSSOF algorithm to obtain the boundary limits of multi-responses optimization. In term of simultaneous C_2 selectivity and yield optimization, the C_2 hydrocarbons selectivity achieves 82.62% ($F_1^{\mathrm{U}}(\boldsymbol{X}^*)$) when the C_2 yield is 2.98% ($F_2^{\mathrm{L}}(\boldsymbol{X}^*)$) at the same independent variables. In the contrary, the optimal C_2 hydrocarbons yield is achieved at 3.93% ($F_2^{\mathrm{U}}(\boldsymbol{X}^*)$), while the corresponding C_2 hydrocarbons selectivity is 59.63% ($F_1^{\mathrm{L}}(\boldsymbol{X}^*)$) at the same independent variables. The correlations indicate an opposing trend between the two responses where the increment of one response lowers the other one and vice versa.

Moreover, variation effect of W_1 and W_2 to the objective functions of CH_4 conversion ($F_1(\boldsymbol{X})$) and C_2 selectivity ($F_2(\boldsymbol{X})$) is depicted in Fig. 3, where W_1 is varied in the range of 0.6–0.99, while consequently W_2 is varied in the range of 0.4–0.01. Increasing W_1 from 0.6 to 0.99 at decreased W_2 from 0.4 to 0.01 leads to increased objective function of CH_4 conversion and simultaneously decreases C_2 selectivity. In addition, Fig. 4 takes into account the variation effect of weighting coefficients to the objective functions of CH_4 conversion ($F_1(\boldsymbol{X})$) and C_2 yield ($F_1(\boldsymbol{X})$). It is shown that decreasing W_1 from 0.0236 to 0 at increased W_2 from 0.9764 to 1 leads to decreased objective function value of CH_4 conversion and simultaneously increases C_2 yield.

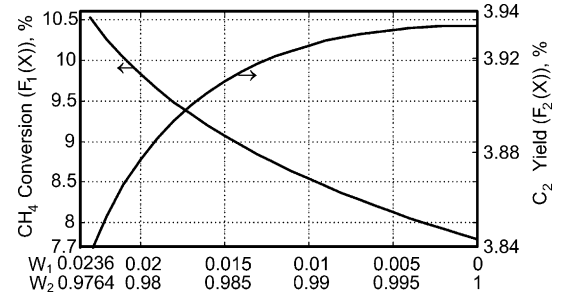

Fig. 4. Relationship of weighting factors variation and objective functions (CH_4 conversion and C_2 yield) in Pareto-optimal solutions.

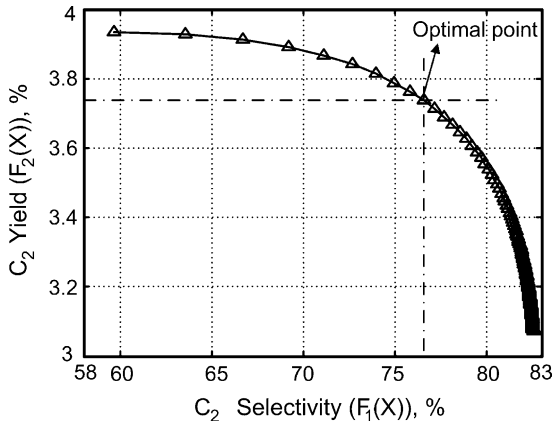

Fig. 5. Pareto-optimal solution for multi-responses optimization of C_2 selectivity and yield in CO_2 OCM process.

3.2.3. Generation of Pareto-optimal solution in multi-responses optimization

It is worth noting that single- and multi-responses optimizations problems are conceptually different. In the multi-responses optimization, there may not be a best solution (global optimum) with respect to both objectives. Instead, there are an entire set of optimal solutions that are evenly good which leads to a situation wherein a set of non-inferior solutions is obtained rather than a unique solution [22,36–37].

Figs. 5–7 depict the Pareto-optimal solutions of the CO_2 OCM process optimization over CaO-MnO/CeO_2 catalyst corresponding to the simultaneous optimization of C_2 selectivity and yield, CH_4 conversion and C_2 selectivity, and CH_4 conversion and C_2 yield, respectively. The trend of the Pareto-optimal solutions shown in the figures coincides with that of the weighting factors variation as depicted in Figs. 2–4. From the figures, it can be shown that if the $F_1(\boldsymbol{X})$ increases, consequently the $F_2(\boldsymbol{X})$ is worsened. Thus, it could not be deduced that any of these non-dominated solutions in the Pareto set is an acceptable final solution. The next task is how to choose a unique final solution. The final solution is important in recommending the suitable operating conditions and catalyst

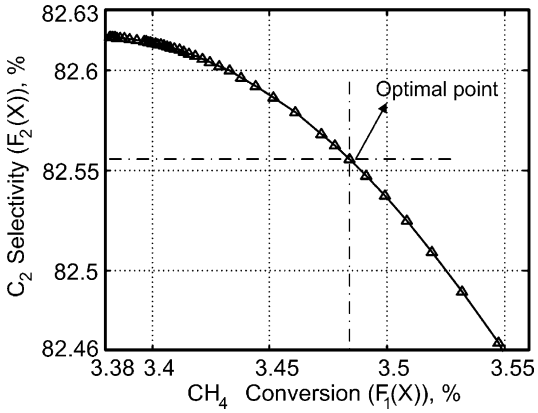

Fig. 6. Pareto-optimal solution for multi-responses optimization of CH_4 conversion and C_2 selectivity in CO_2 OCM process.

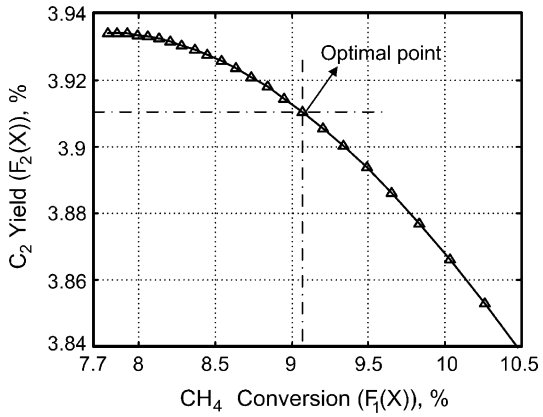

Fig. 7. Pareto-optimal solution for multi-responses optimization of CH_4 conversion and C_2 yield in CO_2 OCM process.

compositions of the process. The selection of the final solution over the entire non-inferior solution requires an additional knowledge of the system, and often, this knowledge is intuitive and non-quantifiable. In this paper, the choice of the final solution is based on the sum of both objective functions, $\Sigma \boldsymbol{F}(\boldsymbol{X})$. As mentioned before, the unique optimum is chosen at maximum of the sum of objective functions. The final criterion means that the unique optimal solution corresponds to the highest C_2 selectivity and yield, CH_4 conversion and C_2 selectivity, or CH_4 conversion and C_2 yield simultaneously. The Pareto set is useful, however, since it narrows the choices and helps to guide the decision maker in selecting the desired operating variables or preferred solution from among the set of Pareto-optimal points.

3.2.4. Location of optimal process parameters and catalyst compositions in multi-responses optimization of CO_2 OCM

Location of the optimal process parameters and the catalyst compositions for the multi-responses optimization of

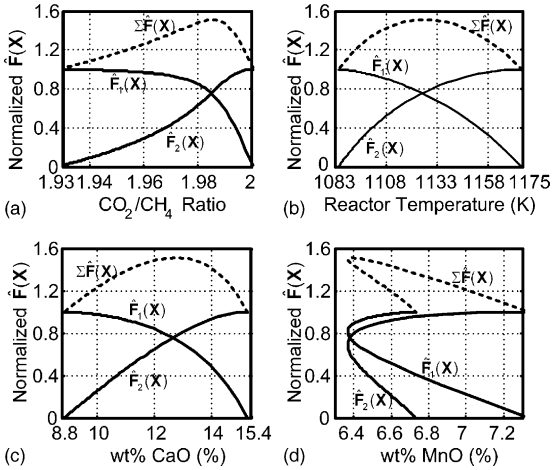

Fig. 8. Location of final optimal conditions for simultaneous C_2 selectivity and yield optimization using maximum normalized $\Sigma \hat{\boldsymbol{F}}(\boldsymbol{X})$ as criterion from Pareto-optimal solution.

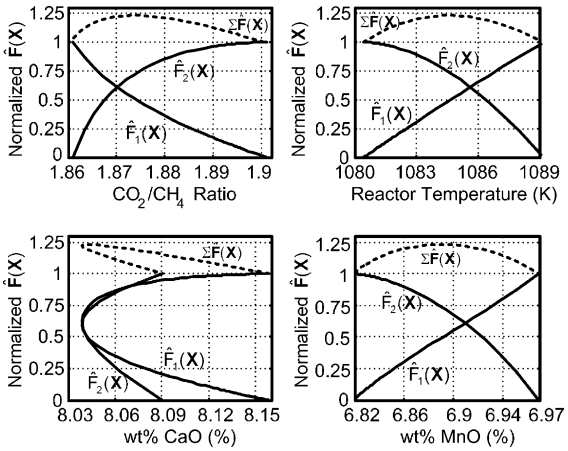

Fig. 9. Location of final optimal conditions for simultaneous CH_4 conversion and C_2 selectivity optimization using maximum normalized $\Sigma\hat{F}(X)$ as criterion from Pareto-optimal solution.

CO_2 OCM are depicted in Figs. 8–10 for C_2 selectivity and yield, CH_4 conversion and C_2 selectivity, and CH_4 conversion and C_2 yield, respectively. The objective functions in this section are presented as the normalized objective functions formulated in Eq. (15). Pertaining to simultaneous optimization of C_2 selectivity and yield, the optimal process parameters results depicted in Fig. 8 are 1.99 and 1127 K for CO_2/CH_4 ratio and reactor temperature, respectively. The simultaneous optimal C_2 selectivity and yield in this optimization is in accordance with the result by Wang et al. [5,7] and Cai et al. [8] at which a high C_2 yield was achieved at higher reactor temperature and high CO_2/CH_4 ratio (about 2). However, the high C_2 selectivity was attained at lower reactor temperature. In addition, the final optimal compositions of CaO-MnO/CeO_2 catalyst are 12.78% and 6.39% for wt.% CaO and wt.% MnO, respectively. Particularly, the unique final maximum C_2 selectivity and yield are included as one of the Pareto-optimal solutions set as revealed in Fig. 5. In fact,

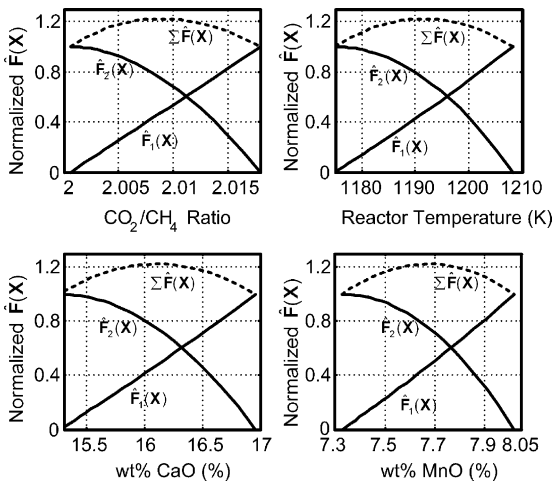

Fig. 10. Location of final optimal conditions for simultaneous CH_4 conversion and C_2 yield optimization using maximum normalized $\Sigma\hat{F}(X)$ as criterion from Pareto-optimal solution.

the optimal values of decision variables are located within the range of the individual response optimization using RSM except for the wt.% MnO.

Fig. 9 takes into account the location of simultaneous maximum CH_4 conversion and C_2 selectivity in which the final optimal conditions are shown at CO_2/CH_4 ratio 1.88 and reactor temperature 1084 K, respectively. Meanwhile, the final optimal catalyst compositions are obtained at 8.04 wt.% CaO and 6.88 wt.% MnO in the CeO_2-supported catalyst. The optimal decision factors of multi-responses optimization of CH_4 conversion and C_2 yield as depicted in Fig. 10 resulted in the final optimal conditions of 2.01 and 1191 K for CO_2/CH_4 ratio and reactor temperature, respectively. The corresponding optimal catalyst compositions are 16.09 wt.% CaO and 7.67 wt.% MnO in the CeO_2-supported catalyst.

3.3. Multi-responses optimization results of CO_2 OCM

3.3.1. Simultaneous optimization of C_2 selectivity and yield

The simultaneous multi-responses optimization results are revealed in Table 5 together with the corresponding optimal independent variables. It is shown that the simultaneous optimal multi-responses are achieved at values of 76.56% and 3.74% for C_2 hydrocarbons selectivity and yield, respectively. In fact, the results are lower than those obtained from the single-response optimization described in Tables 3 and 4. The optimal process parameters and catalyst compositions from the multi-responses optimization are achieved at CO_2/CH_4 ratio and reactor temperature of 1.99 and 1127 K, respectively, and the wt.% CaO and wt.% MnO of 12.78% and 6.39%, respectively. According to the results, the optimal independent variables are located within the range between those from the single-response optimization except for the wt.% MnO in the catalyst as revealed in Fig. 8. The distinct trend of wt.% MnO may be due to the complexity of the optimization problem of the CO_2 OCM process in the numerical computation. It implies that there exist different factors influencing both responses. The reactor temperature has the highest effect indicated by a high diversity in the optimal reactor temperature between multi- and single-responses, while the wt.% MnO has the lowest effect. The interaction between reactor temperature and wt.% CaO has also significantly affected the responses [26].

Pertaining to the relationship between reactor temperature and wt.% CaO, the previous results also indicate that a high C_2 selectivity is achieved at lower reactor temperature and wt.% CaO in the catalyst, while a high C_2 yield is achieved at higher reactor temperature and wt.% CaO in the catalyst. The considerable C_2 hydrocarbons yield at high reactor temperature is related to a high methane conversion. Increasing CaO content in the catalyst enhances the CO_2 adsorption on the catalyst surface due to increasing catalyst basicity and improved the methane conversion, C_2 selectivity and C_2 yield. Interaction of reactor temperature and wt.% CaO in the catalyst (X_2X_3) gives a considerable significant effect towards

Table 5
Simultaneous optimal multi-responses of C_2 selectivity and yield and its corresponding factors location

Simultaneous optimal multi-responses		Corresponding weighting coefficient (W_i)
Response	Maximum value (%)	
C_2 selectivity ($F_1(\boldsymbol{X})$)	76.56	$W_1 = 0.0018$
C_2 yield ($F_2(\boldsymbol{X})$)	3.74	$W_2 = 0.9982$

Location of factors for simultaneous optimal multi-responses	
Factor/independent variable	Optimum value
CO_2/CH_4 ratio (X_1)	1.99
Reactor temperature (X_2) (K)	1127
wt.% CaO in the catalyst (X_3) (%)	12.78
wt.% MnO in the catalyst (X_4) (%)	6.39

C_2 hydrocarbons yield as reported in the previous paper [26]. In fact, a higher reactor temperature leads to enhancement of methane conversion and C_2 hydrocarbons yield but diminished the C_2 hydrocarbons selectivity [26]. Unfortunately, high reactor temperature is not selective to C_2 hydrocarbons. In the case of the high reactor temperature, methane may be largely converted into carbon monoxide rather than C_2 hydrocarbons. Based on this observation, the catalyst plays an important role in promoting the product selectivity to C_2 hydrocarbon and in inhibiting the reaction to CO and water. According to thermodynamics equilibrium calculations, the equilibrium constant increases with the reactor temperature for an endothermic reaction such as CO_2 OCM. The larger equilibrium constant shifts the reaction to the right and increases the equilibrium conversion.

3.3.2. Simultaneous optimization of CH_4 conversion and C_2 selectivity

The simultaneous CH_4 conversion and C_2 selectivity optimization results are revealed in Table 6. In this table, the simultaneous optimal CH_4 conversion and C_2 hydrocarbons selectivity are achieved at values of 3.48% and 82.56%, respectively. The corresponding optimal process parameters and catalyst compositions are achieved at the CO_2/CH_4 ratio and reactor temperature of 1.88 and 1084 K, respectively, and the wt.% CaO and wt.% MnO of 8.04% and 6.88%, respectively. The operating conditions results can also be shown in Fig. 9. In fact, the simultaneous optimal C_2 selectivity is closed to that of the optimal single-response. In the single-response optimization, the C_2 selectivity has a maximum performance at low reactor temperature, while a high CH_4 conversion is achieved at high reactor temperature. However, the simultaneous optimization of CH_4 conversion and C_2 selectivity is significantly affected on lowering the optimal reactor temperature. It is implied that a lower reactor temperature leads to a higher C_2 selectivity, while a higher reactor temperature leads to a high C_2 yield.

3.3.3. Simultaneous optimization of CH_4 conversion and C_2 yield

Table 7 demonstrates the multi-responses optimization of simultaneous CH_4 conversion and C_2 yield including its corresponding optimal conditions. It is shown that the simultaneous optimal CH_4 conversion and C_2 yield responses are obtained at 9.07% and 3.91%, respectively. From Table 7 it is revealed that the simultaneous optimal CH_4 conversion and C_2 hydrocarbons yield are achieved at CO_2/CH_4 ratio and reactor temperature of 2.01 and 1191 K, respectively, and wt.% CaO and wt.% MnO of 16.09% and 7.67%, respectively. In fact, the simultaneous optimal CH_4 conversion and C_2 yield are attained at high reactor temperature (1191 K). It is suggested that both CH_4 conversion and C_2 yield are en-

Table 6
Simultaneous optimal multi-responses of CH_4 conversion and C_2 selectivity and its corresponding factors location

Simultaneous optimal multi-responses		Corresponding weighting coefficient (W_i)
Responses	Maximum value (%)	
CH_4 conversion ($F_1(\boldsymbol{X})$)	3.48	$W_1 = 0.966$
C_2 selectivity ($F_2(\boldsymbol{X})$)	82.56	$W_2 = 0.034$

Location of factors for simultaneous optimal multi-responses	
Factor/independent variable	Optimum value
CO_2/CH_4 ratio (X_1)	1.88
Reactor temperature (X_2) (K)	1084
wt.% CaO in the catalyst (X_3) (%)	8.04
wt.% MnO in the catalyst (X_4) (%)	6.88

Table 7
Simultaneous optimal multi-responses of CH_4 conversion and C_2 yield and its corresponding factors location

Simultaneous optimal multi-responses		Corresponding weighting coefficient (W_i)
Responses	Maximum value (%)	
CH_4 conversion ($F_1(\boldsymbol{X})$)	9.07	$W_1 = 0.015$
C_2 yield ($F_2(\boldsymbol{X})$)	3.91	$W_2 = 0.985$

Location of factors for simultaneous optimal multi-responses

Factor	Optimum value
CO_2/CH_4 ratio (X_1)	2.01
Reactor temperature (X_2) (K)	1191
wt.% CaO in the catalyst (X_3) (%)	16.09
wt.% MnO in the catalyst (X_4) (%)	7.67

Table 8
Result validations of the final optimal point in the multi-responses optimization of C_2 selectivity and yield

C_2 yield (%)			C_2 selectivity (%)		
$F_{\text{multi-responses}}$	$F_{\text{experimental}}$	% Relative error*	$F_{\text{multi-responses}}$	$F_{\text{experimental}}$	% Relative error*
3.74	3.76	0.56	76.56	65.27	17.30
3.74	3.39	10.22	76.56	63.56	20.45
3.74	3.49	7.30	76.56	67.92	12.72
3.74	3.35	11.78	76.56	67.21	13.92
Average relative error	7.47		16.10		

Note: Operating conditions: CO_2/CH_4 ratio, 1.99; reactor temperature, 1127 K; catalyst, 12.78 wt.% CaO-6.39 wt.% MnO/CeO_2.

* $\%\,\text{Relative error} = \left(\frac{|F_{\text{experiment}} - F_{\text{multi-responses}}|}{F_{\text{experiment}}}\right) \times 100\%$.

hanced at a high reactor temperature as described elsewhere [26].

3.4. Results validation and benefit of multi-responses optimization in CO_2 OCM process

In this optimization, there are three multi-responses optimization combinations where two responses are simultaneously applied for each combination, i.e. C_2 selectivity and yield, CH_4 conversion and C_2 selectivity, and CH_4 conversion and C_2 yield. In this case, the optimization of C_2 selectivity and yield is chosen for the recommendation in order to suggest the operating conditions and the catalyst compositions. The reason for this choice is that C_2 yield involves CH_4 conversion and C_2 selectivity as mentioned in the previous section. It is expected that the simultaneous optimization of C_2 selectivity and yield takes into account the high performance of CH_4 conversion, C_2 selectivity and C_2 yield simultaneously.

Moreover, the experimental validations of CO_2 OCM process with respect to the multi-responses optimization of C_2 selectivity and yield are revealed in Table 8. In this validation, the C_2 selectivity and yield at the final optimal point are compared with those from experimental data at the similar conditions. From the table, it is shown that the average relative error for C_2 selectivity and yield are 16.10% and 7.47%, respectively. However, it is shown that the performances of the experimental works are still lower than that from the multi-responses optimization.

Indeed, the empirical modeling using RSM combined with multi-responses optimization is useful for optimizing the CO_2 OCM process in certain ranges of independent variables before kinetic studies are implemented. The empirical modeling and the multi-responses optimization method is useful for designing a catalyst as well as exploring the interaction among the variables towards the process performances. The results of the hybrid multi-responses optimization can be used to recommend the operating conditions and catalyst compositions for further experimental works in CO_2 OCM process especially in the kinetic studies.

4. Conclusions

A new multi-responses optimization algorithm using Weighted Sum of Squared Objective Functions technique to obtain Pareto-optimal solutions was developed. A unique optimal point among the Pareto set was resulted by considering an additional optimal criterion. The algorithm successfully optimized CO_2/CH_4 ratio, reactor temperature, wt.% CaO and wt.% MnO in the catalyst in order to maximize two responses simultaneously, i.e. C_2 hydrocarbons selectivity and yield, CH_4 conversion and C_2 selectivity, as well as CH_4 conversion and C_2 yield. The hybrid numerical approach

combined single-response modeling using Response Surface Methodology with the WSSOF technique for solving multi-responses optimization. In this paper, the WSSOF technique was successfully implemented to solve the multi-responses optimization in CO_2 OCM process.

The operating conditions and catalyst compositions from multi-responses optimization of C_2 selectivity and yield within the Pareto-optimal solutions were chosen as recommendation for the CO_2 OCM process. This choice was based on the fact that the C_2 yield was taken into account both CH_4 conversion and C_2 selectivity. The maximum values of 76.56% and 3.74% for C_2 hydrocarbons selectivity and yield, respectively, were achieved with respect to the optimal independent variables: CO_2/CH_4 ratio = 1.99, reactor temperature = 1127 K, wt.% CaO = 12.78% and wt.% MnO = 6.39%. The optimal C_2 selectivity and yield from the validation results closed to those from multi-responses optimization with small relative errors. The results of the multi-response optimization could be used to facilitate in recommending suitable operating conditions and catalyst compositions for the CO_2 OCM process.

Acknowledgment

The authors would like to express their sincere gratitudes to the Ministry of Science, Technology and Innovation (MOSTI), Malaysia, for the financial support received under the Project No. 02-02-06-0016 EA099.

References

[1] T. Suhartanto, A.P.E. York, A. Hanif, H. Al-Megren, M.L.H. Green, Potential utilisation of Indonesia's Natuna natural gas field via methane dry reforming to synthesis gas, Catal. Lett. 71 (2001) 49–54.
[2] K. Asami, T. Fujita, K. Kusakabe, Y. Nishiyama, Y. Ohtsuka, Conversion of methane with carbon dioxide into C_2 hydrocarbons over metal oxides, Appl. Catal. A. 126 (1995) 245–255.
[3] K. Asami, K. Kusakabe, N. Ashi, Y. Ohtsuka, Synthesis of ethane and ethylene from methane and carbon dioxide over praseodymium oxide catalysts, Appl. Catal. A. 156 (1997) 43–56.
[4] Y. Wang, Y. Ohtsuka, CaO-ZnO catalyst for selective conversion of methane to C_2 hydrocarbons using carbon dioxide as the oxidant, J. Catal. 192 (2000) 252–255.
[5] Y. Wang, Y. Ohtsuka, Mn-based binary oxides as catalyst for the conversion of methane to C_{2+} hydrocarbon with carbon dioxide as an oxidant, Appl. Catal. A. 219 (2001) 183–193.
[6] Y. Wang, Y. Takahashi, Y. Ohtsuka, Carbon dioxide-induced selective conversion of methane to C_2 hydrocarbons on CeO_2 modified with CaO, Appl. Catal. A. 172 (1998) L203–L206.
[7] Y. Wang, Y. Takahashi, Y. Ohtsuka, Carbon dioxide as oxidant for the conversion of methane to ethane and ethylene using modified CeO_2 catalyst, J. Catal. 186 (1999) 160–168.
[8] Y. Cai, L. Chou, S. Li, B. Zhang, J. Zhao, Selective conversion of methane to C_2 hydrocarbons using carbon dioxide over Mn-$SrCO_3$ catalysts, Catal. Lett. 86 (2003) 191–195.
[9] Istadi, N.A.S. Amin, Screening of MgO- and CeO_2-based catalysts for carbon dioxide oxidative coupling of methane to C_{2+} hydrocarbons, J. Nat. Gas Chem. 13 (2004) 23–35.
[10] T. Hattori, S. Kito, Artificial intelligence approach to catalyst design, Catal. Today 10 (1991) 213–222.
[11] T. Hattori, S. Kito, Neural network as a tool for catalyst development, Catal. Today 23 (1995) 347–355.
[12] Z.Y. Hou, Q.L. Dai, X.Q. Wu, G.T. Chen, Artificial neural network aided design of catalyst for propane ammoxidation, Appl. Catal. A. 161 (1997) 183–190.
[13] K. Huang, F.Q. Chen, D.W. Lü, Artificial neural network-aided design of a multi-component catalyst for methane oxidative coupling, Appl. Catal. A. 219 (2001) 61–68.
[14] D. Wu, Y. Li, Y. Shi, Z. Fang, D. Wu, L. Chang, Effects of the calcination conditions on the mechanical properties of a PCoMo/Al_2O_3 hydrotreating catalyst, Chem. Eng. Sci. 57 (2002) 3495–3504.
[15] A.L. Larentis, N.S. de Resende, V.M.M. Salim, J.C. Pinto, Modeling and optimization of the combined carbon dioxide reforming and partial oxidation of natural gas, Appl. Catal. A. 215 (2001) 211–224.
[16] K. Huang, X.L. Zhan, F.Q. Chen, D.W. Lü, Possibility of direct conversion of CH_4 and CO_2 to high-value products, Chem. Eng. Sci. 58 (2003) 81–87.
[17] D. de Faveri, P. Torre, P. Perego, A. Converti, Optimization of xylitol recovery by crystallization from synthetic solutions using Response Surface Methodology, J. Food Eng. 61 (2004) 407–412.
[18] R. Muralidhar, S.N. Gummadi, V.V. Dasu, T. Panda, Statistical analysis on some critical parameters affecting the formation of protoplasts from the mycelium of penicillium griseovulfum, Biochem. Eng. J. 16 (2003) 229–235.
[19] A.D. Nandasana, A.K. Ray, S.K. Gupta, Dynamic model of an industrial steam reformer and its use for multi-objective optimization, Ind. Eng. Chem. Res. 42 (2003) 4028–4042.
[20] W. Zhao, D. Chen, S. Hu, Optimizing operating conditions based on ANN and modified gas, Comp. Chem. Eng. 24 (2000) 61–65.
[21] S. Nandi, Y. Badhe, J. Lonari, U. Sridevi, B.S. Rao, S.S. Tambe, B.D. Kulkarni, Hybrid process modeling and optimization strategies integrating neural networks/support vector regression and genetic algorithms: study of benzene isopropylation on Hbeta catalyst, Chem. Eng. J. 97 (2004) 115–129.
[22] Z. Zhang, K. Hidajat, A.K. Ray, Multi-objective optimization of SMB and varicol process for chiral separation, AIChE J. 48 (2002) 2800–2816.
[23] D.C. Montgomery, Design and Analysis of Experiments, John Wiley & Sons, New York, 2001.
[24] G.M. Clarke, R.E. Kempson, Introduction to the Design and Analysis of Experiments, Arnold, London, 1997.
[25] J.A. Cornell, How to Apply Response Surface Methodology, American Society for Quality Control, Wisconsin, 1990.
[26] Istadi, N.A.S. Amin, Optimization of process parameters and catalyst compositions in CO_2 oxidative coupling of methane over CaO-MnO/CeO_2 catalyst using Response Surface Methodology. Fuel Process. Technol., in press.
[27] T.F. Edgar, D.M. Himmelblau, L.S. Lasdon, Optimization of Chemical Processes, McGraw-Hill Inc., New York, 2001.
[28] W. Yu, K. Hidajat, A.K. Ray, Application of multi-objective optimization in the design and operation of reactive SMB and its experimental verification, Ind. Eng. Chem. Res. 42 (2003) 6823–6831.
[29] V.S. Summanwar, V.K. Jayaraman, B.D. Kulkarni, H.S. Kusumakar, K. Gupta, J. Rajesh, Solution of constrained optimization problems by multi-objective genetic algorithm, Comp. Chem. Eng. 26 (2002) 1481–1492.
[30] The MathWorks, MATLAB Optimization Toolbox User's Guide, The MathWorks Inc., Natick, MA, 2001.
[31] E.A. Youness, Characterization of efficient solutions of multi-objective E-convex programming problems, Appl. Math. Comp. 151 (2004) 755–761.
[32] D. Ko, I. Moon, Multi-objective optimization of cyclic adsorption processes, Ind. Eng. Chem. Res. 41 (2002) 93–104.

[33] M.L. Luyben, C.A. Floudas, Analyzing the interaction of design and control. 1. A multi-objective framework and application to binary distillation synthesis, Comp. Chem. Eng. 18 (1994) 933–969.
[34] W. Warsito, L.S. Fan, Neural network multi-criteria optimization image reconstruction technique (NN-MOIRT) for linear and non-linear process tomography, Chem. Eng. Process. 42 (2003) 663–674.
[35] Q. Xiong, A. Jutan, Continuous optimization using a dynamic simplex method, Chem. Eng. Sci. 58 (2003) 3817–3828.
[36] M.K. Krokida, C.T. Kiranoudis, Pareto design of fluidized bed dryers, Chem. Eng. J. 79 (2000) 1–12.
[37] C.M. Silva Jr., E.C. Biscaia, Genetic algorithm development for multi-objective optimization of batch free-radical polymerization reactors, Comp. Chem. Eng. 27 (2003) 1329–1344.